

# Synchronous Membrane Potential Fluctuations in Neurons of the Cat Visual Cortex

Ilan Lampl\*, Iva Reichova, and David Ferster  
Department of Neurobiology and Physiology  
Northwestern University  
Evanston, Illinois 60208

## Summary

We have recorded intracellularly from pairs of neurons less than 500  $\mu\text{m}$  distant from one another in V1 of anesthetized cats. Cross-correlation of spontaneous fluctuations in membrane potential revealed significant correlations between the cells in each pair. This synchronization was not dependent on the occurrence of action potentials, indicating that it was not caused by mutual interconnections. The cells were synchronized continuously rather than for brief epochs. Much weaker correlations were found between the EEG and intracellular potentials, suggesting local, rather than global, synchrony. The highest correlation occurred among cells with similar connectivity from the LGN and similar receptive fields. During visual stimulation, correlations increased when both cells responded to the stimulus and decreased when neither cell responded.

## Introduction

Traditional studies of cortical information processing, whether centered in sensory or motor systems, have focused primarily on the activity of single neurons. It has long been thought, however, that a more complete understanding of the brain will come from recording activity from populations of neurons, rather than from one neuron at a time. In many sensory and motor areas, there is now evidence that the relative timing of spikes in groups of neurons can encode information beyond what is carried by the spike trains of single cells.

In the retina (Meister, 1996) and cortex (Ghose et al., 1994), for example, synchronous spikes in adjacent pairs of neurons can define a receptive field consisting of small overlapping regions of the receptive fields of the two individual cells. In the visual cortex, it has been suggested that synchronous firing in cells with widely separated receptive fields can signal that the two fields are being stimulated by parts of the same object (Engel et al., 1991b). In the auditory system, synchronous firing signals the duration of stimuli even while the firing rates of individual neurons have returned to spontaneous levels (deCharms and Merzenich, 1996). Changes in neuronal synchrony in the motor system have been seen to anticipate specific behavioral states (Vaadia et al., 1995; Murthy and Fetz, 1996; Riehle et al., 1997). In the rat trigeminal somatosensory system, oscillatory synchrony

among the thalamus, cortex, and brainstem reliably predicted exploratory whisker twitching (Nicolleis et al., 1995).

Within the visual cortex, correlated spike activity has been observed under different conditions (Toyama et al., 1981a, 1981b; Ts'o et al., 1986; Engel et al., 1991a, 1991c; Freiwald et al., 1995; Nowak et al., 1995). Because they rely exclusively on extracellular recordings, however, these studies do not reveal the subthreshold events leading to the synchrony. For example, the subthreshold synaptic inputs to cells with highly correlated firing could be highly uncorrelated for long stretches but punctuated by brief synchronous bursts of suprathreshold input. Alternatively, synaptic inputs could be correlated for long, continuous periods. In addition, synchronous inputs could interact strongly with a neuron's intrinsic firing properties to shape the exact nature of the correlations in output (Mainen and Sejnowski, 1995; Stevens and Zador, 1998). In general, then, what pattern of correlation in the inputs to two cells is required to generate a particular pattern of spike synchrony? A first step in understanding the sources of correlated firing is to study correlations in subthreshold activity.

In this study, we have recorded intracellularly in the cat visual cortex from pairs of neurons with overlapping receptive fields and found that subthreshold fluctuations in membrane potential were significantly correlated in every pair, in many pairs to a very high degree. Several important features of the subthreshold synchrony were observed. (1) The cells were synchronized not only during the occurrence of synchronous spikes, but continuously during the entire recording period. (2) The spontaneous synchronized activity was rarely accompanied by oscillations. (3) In most pairs, the time lag between the synchronous activity in the two cells was less than 5 ms. (4) Correlation was also stronger between cells with similar synaptic connectivity (mono- or polysynaptic) from relay cells of the LGN. (5) The spontaneous correlation was stronger in pairs of neurons with similar receptive field type (simple or complex) than in pairs with dissimilar types. (6) Increasing the firing rate of two highly correlated cells (by injecting positive current into both cells) evoked synchronized firing. The width of the resulting spike correlograms was three to ten times narrower than the width of the membrane potential correlogram (four pairs). (7) Visual stimuli that simultaneously activated two complex cells evoked stronger and temporally more precise correlations than did stimuli that activated neither cell (two pairs).

These observations, that subthreshold inputs to nearby neurons are strongly correlated and that the correlations depend on the receptive field properties and connectivity of the neurons, have significant implications for the role and origins of synchronized activity.

## Results

We recorded from 64 pairs of cells, for a total of 114 cells (some cells were members of more than one pair).

\* To whom correspondence should be addressed (e-mail: i-lampl@nwu.edu).

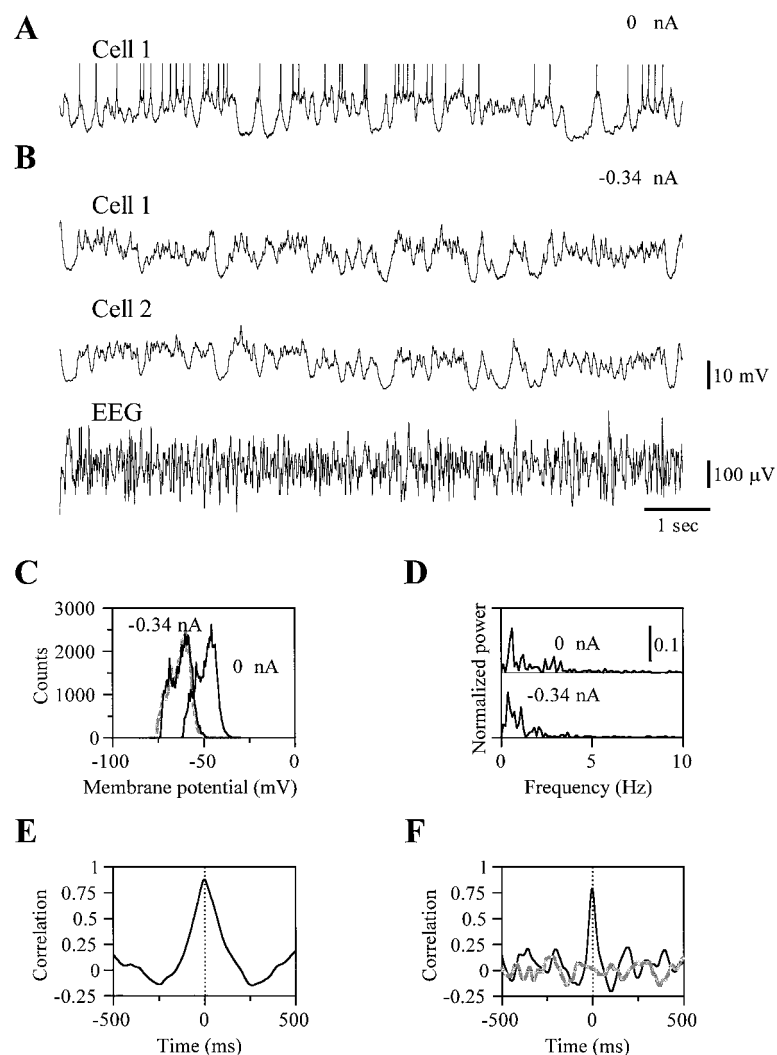


Figure 1. Spontaneous Membrane Potential Fluctuations Are Synchronized in Neighboring Cortical Cells

(A) Spontaneous activity (10 s) recorded intracellularly from a visual cortical neuron. Spikes are truncated.

(B) Simultaneously recorded membrane potentials from two cells, along with the EEG. The top trace (cell 1) is the same cell as in (A), but with a steady current ( $-0.34$  nA) injected to suppress firing. Cell 2 was located approximately  $500 \mu\text{m}$  from cell 1. The EEG was recorded from cranial screws  $1.5$  cm distant from the recorded cells. The two neurons are highly synchronized.

(C) Membrane potential histograms for cell 1 constructed from 30 s of data recorded with and without injected current. The  $0$  nA histogram is copied in gray and shifted to the left for comparison with the  $-0.34$  nA histogram.

(D) Power spectra for 30 s traces from cell 1 obtained with and without current injection. The similarities in the two histograms and in the two power spectra suggest that the membrane potential fluctuations are not critically dependent on the intrinsic voltage-sensitive properties of the cell.

(E) Cross-correlation between cell 1 and cell 2 (with cell 1 as the reference).

(F) Cross-correlogram between digitally high-pass filtered ( $5$  Hz Butterworth) records from cell 1 and cell 2 (black curve), together with the cross-correlogram between high-pass filtered recordings of cell 1 and the EEG (gray curve).

The horizontal distance between the cells in each pair was less than  $500 \mu\text{m}$ ; the average vertical distance between them was  $350 \pm 39 \mu\text{m}$  (all means are reported as mean  $\pm$  SEM). In 17 pairs, receptive fields were mapped by hand-held projector and were found to be at least partially overlapping. The correlation analysis described in this study was performed primarily in the absence of spiking. In some pairs, we reduced the firing rate by continuous injection of hyperpolarizing current. Cells that still had high firing frequency with an injection of  $-2$  nA or greater were excluded from analysis, as were cells with slow drifts in the membrane potential or with heartbeat or respiration artifacts. When persistent spindle activity was present in the EEG, we sometimes observed similar waves in the intracellular recordings. These pairs were also excluded (see below).

In contrast to recordings obtained *in vitro*, the membrane potential of neurons recorded *in vivo* shows vigorous spontaneous synaptic activity (Pare et al., 1998). This activity is characterized in some of our recorded cells by low-frequency shifts between two distinct levels of the membrane potential separated from one another by  $10$  mV or more. These "up" and "down" states have

been previously described in striatal neurons (Wilson and Kawaguchi, 1996; Stern et al., 1998) and are also evident in recordings from cerebral cortex (Steriade et al., 1993). More specifically, they can appear in V1 (Douglas et al., 1991) where visual stimulation can affect the statistics of the membrane potential shifts (Ferster and Carandini, 1996).

An example of large spontaneous fluctuations in membrane potential is shown for a cortical cell in Figure 1A. The cell fires relatively slowly ( $\sim 4/\text{s}$ ), and the membrane potential swings through a  $15$  mV range, spending much of its time in a relatively depolarized state. Smaller amplitude, fast fluctuations, which occasionally give rise to spikes, ride on top of the depolarized state but are largely absent from the hyperpolarized state.

We found large variability in the pattern of the spontaneous fluctuations: the depolarized states range in duration from  $50$  to  $1000$  ms and show large variability in amplitude. It has been suggested that these fluctuations either have synaptic origins (Wilson and Kawaguchi, 1996; Plenz and Kitai, 1998; Stern et al., 1998) or that they arise from intrinsic voltage-sensitive mechanisms (Ferster and Carandini, 1996; Wilson and Kawaguchi,

1996). If the latter, hyperpolarization of the membrane by current injection should change the temporal pattern of activity. When negative current was injected into cell 1 in Figure 1A, a mean hyperpolarization of 15.6 mV was induced (Figure 1B, upper trace) and the cell ceased to fire, but the large membrane potential fluctuations remained and were very similar in character to the activity recorded without injected current: the membrane potential histograms in Figure 1C show similar shapes, except for the clear, current-induced shift in the mean level. Neither did the current injection have a significant effect on the dynamics of the fluctuations in membrane potential, as can be observed from the similarities of the power spectra plotted in Figure 1D. Similar results to Figure 1 were obtained in a total of 15 cells, suggesting that the subthreshold membrane potential fluctuations arise not from intrinsic voltage-dependent mechanism, but largely from synaptic input.

A second observation points to the synaptic origin of the spontaneous activity: the activity in the cell in Figure 1A was highly synchronized with the activity in a second cell located less than 500  $\mu\text{m}$  away (Figure 1B). Almost every large swing in membrane potential in one cell is accompanied by a similar event in the other cell. Since neither cell spiked during the recordings, the source of these events must be extrinsic to the two cells, and not, for example, recurrent synaptic connections between them or voltage sensitive mechanisms intrinsic to either cell.

If the large spontaneous events are synaptic, the question immediately arises as to the location of the presynaptic neurons. Are they in V1 near the recorded cell, or perhaps in other cortical areas, or outside the cortex entirely? If the synchrony encompassed different cortical areas, for example, we would expect to find the recorded cells to be synchronized with the electroencephalogram (EEG). We therefore recorded the EEG in the opposite hemisphere (between electrodes at L3, P5 and L3, A10) at a distance of approximately 1.5 cm from the intracellular electrodes (Figure 1B, third trace): there is no strong correlation between the EEG and intracellularly recorded membrane potentials.

To quantitate the extent of the synchrony between the cells in a pair and between the cells and the EEG, we computed the cross-correlation between the signals (Figures 1E and 1F). The peak of the correlogram of the two cells (Figure 1E) is high (0.87), indicating that a large proportion of the variance of the two traces is synchronized. Note that the amplitude of the cross-correlogram reflects only the degree of synchrony between traces and not their absolute amplitudes since each trace was first normalized by its standard deviation (see Experimental Procedures). The correlogram is centered around zero time delay, indicating a near-zero time shift between the membrane potential fluctuations in the two cells.

The correlation between the membrane potential of cell 1 and the EEG (Figure 1F, gray line) is much weaker than that between the cells (Figure 1E). There is, however, one complication inherent in comparing the cell-cell correlations and cell-EEG correlations: the EEG signal was high-pass filtered with a cutoff frequency of 1 Hz, whereas the intracellular potentials were not. To

compare the cell-to-cell and the cell-to-EEG correlations more fairly, therefore, we digitally high-pass filtered the intracellular potentials with a cutoff frequency of 5 Hz and recalculated the cell-to-cell correlation (Figure 1F, black line). The cross-correlation curve after filtering is narrower, as expected from exclusion of low frequencies. Nevertheless, the strength of correlation between the cells after filtering (0.79) is almost as high as that for the raw data. The synchronized activity in the cells is therefore not limited to low-frequency membrane potential fluctuations.

The correlation within a single pair of neurons often changed over time. In Figure 2A, the membrane potential from one cell pair is shown for three different 1 s epochs taken from a 30 s recording. The cross-correlograms for these epochs are shown in Figure 2B. The cells were most strongly correlated during T2 (middle traces in Figure 2A); both cells in the pair either depolarized or hyperpolarized simultaneously. In the other epochs (T1 and T3), some potentials that developed in one cell were absent from the other. These changes in synchrony are reflected in the peak amplitude of the corresponding correlograms (0.54, 0.74, and 0.33 for T1, T2, and T3).

The variability in synchrony over time for the full 30 s of recording is shown in Figure 2C, where the peaks of the cross-correlograms constructed from each 1 s epoch are plotted as a function of time. The considerable variability in the extent of synchrony indicates short-term dynamic changes in network activity. On a longer time scale, however, synchrony is more stable: the cross-correlation calculated from the entire 30 s epoch (Figure 2D, black line) differs little from that of other 30 s records (data not shown).

Among the different cell pairs, we found large variability in the width and peak of the cross-correlations. The range of variability is illustrated for four cell pairs in Figure 3. The pair in 3A, for example, showed minimal synchronization: the correlogram from a full 30 s of data (thick black line) shows only a small peak (amplitude: 0.15), and the correlogram from the illustrated 2 s traces showed no clear peak at all. The second pair of cells (Figure 3B) is more synchronized, as can be seen by inspecting the traces, and the correlograms calculated both from the 2 s traces and from the full 30 s of recordings show a clear peak (amplitude: 0.39). The third pair of cells (Figure 3C) is more correlated still (correlogram peak amplitude: 0.62), even though the amplitude of the membrane potential fluctuations in each of the two cells is smaller than that of the second cell in Figure 3B. Finally, the cells of the last pair (Figure 3D) were extremely well synchronized (correlogram peak amplitude: 0.83) with the two traces appearing almost identical.

A summary of the variability in correlation among the cell pairs is shown in Figure 4A. For each of the 64 correlograms, we measured the peak absolute value within a time window of  $\pm 200$  ms from zero lag. The average absolute value of the correlation strength was  $0.40 \pm 0.02$  (range: 0.11 to 0.83). Five pairs were negatively correlated with an average strength of  $-0.14 \pm 0.01$ . That is, a depolarization in one cell was associated most often with a hyperpolarization in the other. The amplitudes of these negative correlations were at the

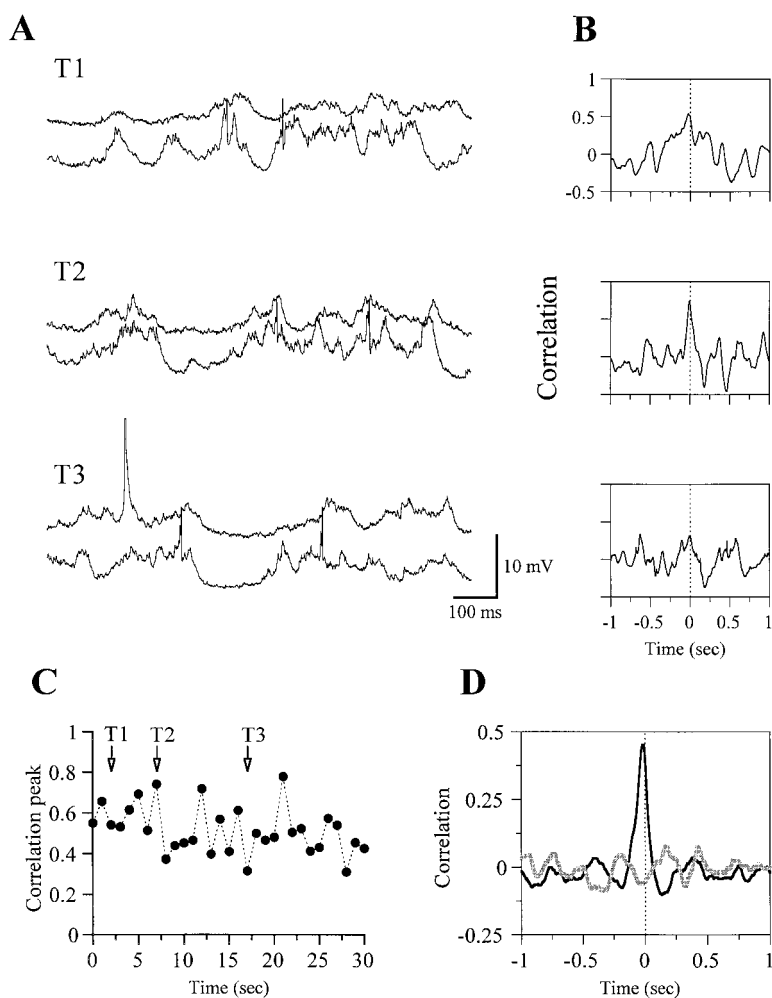


Figure 2. Changes with Time in the Extent of Subthreshold Synchrony between Cells in a Pair

(A) Traces (1 s) recorded simultaneously from two cells at three different times.

(B) Normalized cross-correlograms for each pair of traces in (A) (upper cell as reference). A large variability in the degree of synchrony over time can be observed.

(C) The peak values of the normalized cross-correlograms calculated from 30 consecutive 1 s epochs. Arrows point to the three epochs shown in (A).

(D) Cross-correlogram of the entire 30 s (black curve). The gray curve is the cross-correlogram of the same data after 1 s epochs of the second trace were randomly shuffled.

low end of the range, however, and of these five, four had large delays ( $135 \pm 4$  ms). For comparison, a histogram of the peak correlation between one cell in each pair and the EEG is also plotted in Figure 4A. These correlations are much weaker than the correlations between cells (mean absolute value:  $0.11 \pm 0.01$ ).

The range of the widths of the cell-cell cross-correlograms was large (8 to 92 ms, mean  $48 \pm 2$  ms, measured at half amplitude), and the widths were related to correlation strength such that pairs that were more synchronized tended to have broader correlation (Figure 4B). The time lag between the cells was usually close to zero (Figure 4C), with 80% of the pairs having lags smaller than 5 ms. The median time to peak was 2.8 ms.

#### Measures of Random Correlation

An important question raised by any observation of correlated signals is whether the correlations are statistically significant. Even if the membrane potential of the two cells fluctuated completely independently, some synchrony is bound to occur simply by chance. To assess the amount of correlation that we would expect to appear between two completely independent cells, we constructed shuffled correlograms for each pair (Figures 2D and 3A–3D, gray lines). The shuffled correlogram was

constructed from the same 30 s of data as the solid curve in each case, but with 1 s portions of the second cell chosen in random order with respect to the first. The shuffled correlograms contain no obvious peak at the time of the peak in the nonshuffled correlogram, indicating that the correlations we have observed do not occur by chance.

As a further measure of the significance of the peak value of the correlograms, we repeated the shuffling procedure 250 times with a different shuffling sequence each time. We then measured the value of these 250 shuffled correlograms at the time lag of the peak of the unshuffled correlogram. For no pair of cells did any of these 250 values exceed the amplitude of the peak of the unshuffled correlogram. In all 64 pairs, therefore, the correlations observed were significant to the  $p < 0.004$  level. We also performed the shuffling procedure for the correlations between one cell in each pair and the EEG and found that 57 of the 64 correlation peaks were significant to the  $p < 0.004$  level.

#### The Properties of Synchronized Neurons

What distinguishes cell pairs with a high degree of synchrony? Might they be located in particular layers of the cortex? Do they have similar functional properties? To

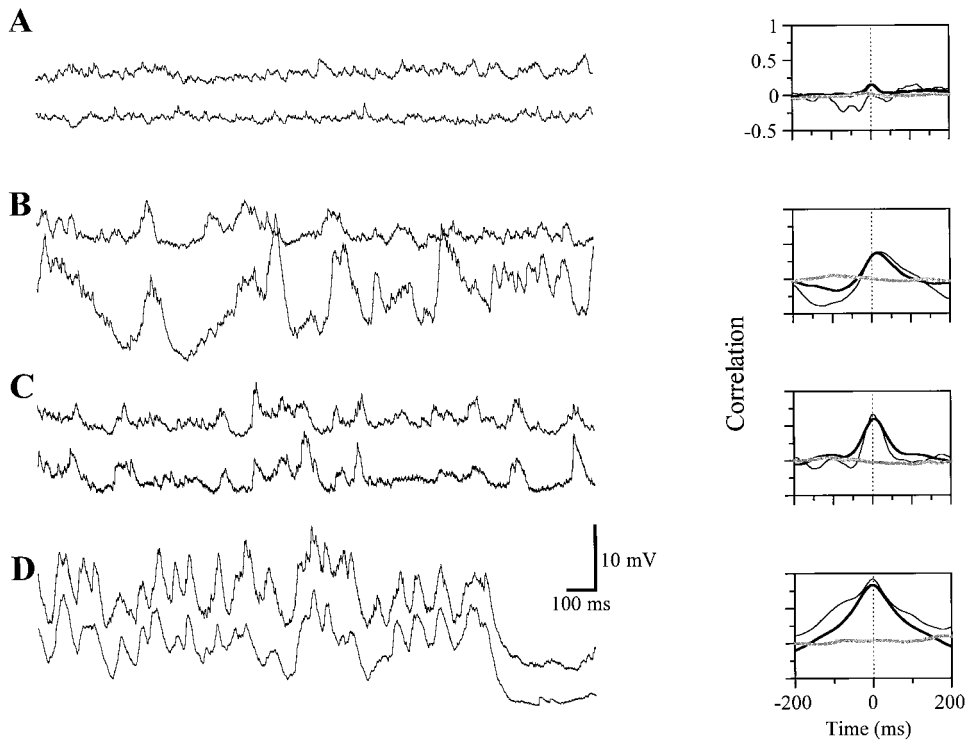


Figure 3. Variability among Cell Pairs in the Extent of Subthreshold Synchrony

Left: 2 s simultaneous recordings from four different pairs of cells.

Right: cross-correlograms of the traces illustrated on the left (thin curves), together with cross-correlograms of 30 s recordings (thick curves), and cross-correlograms of the same 30 s recordings after shuffling (gray curves).

address this question, we characterized the recorded cells and compared their properties to the peaks of their cross-correlograms.

#### *Latency of the Response to LGN Stimulation*

It has been shown previously that only some cells in the primary visual cortex receive monosynaptic input from the LGN, while others receive only polysynaptic input via other cortical interneurons. The two groups of cells differ in their latencies to LGN stimulation (Figure 5A), with monosynaptically connected cells having shorter latencies. While there is some overlap in latency between the two populations (Ferster and Lindstrom, 1983), most cells with monosynaptic connections have latencies shorter than 2.5 ms, and those with only polysynaptic connections have latencies longer than 2.5 ms (Ferster and Lindstrom, 1983; Martin and Whitteridge, 1984a, 1984b). The distribution of latencies to LGN stimulation in 110 cells is shown in Figure 5B. We divided the population into two groups, "m" and "p," depending on whether their latencies were greater or less than 2.5 ms. Consistent with this classification is our observation that the short latency responses jittered much less than the long latency responses (Figure 5A). The cell pairs in which latencies were measured for both cells (49 pairs) were assigned to three groups, in which both cells received mono- or polysynaptic input (m/m and p/p) or one cell received monosynaptic and the other cell polysynaptic input (m/p). The peak correlation for all pairs in a group were then averaged (Figure 5C). The two homogenous groups (m/m and p/p) had significantly

larger synchrony (0.44 and 0.57) than the heterogeneous group (0.26). No difference in correlation width was found between the different populations. Although we used 2.5 ms as the dividing line between mono- and polysynaptic groups, the exact number was not critical to the results. We found that separating the cells at any time between 2.0 ms and 2.5 ms revealed very similar statistical results (data not shown). Thus, the synchrony in the visual cortex is higher among cells with similar connectivity from the LGN than it is among cells with different connectivity.

#### *Receptive Field Type*

To identify receptive field types from the response to drifting gratings, we compared the mean component (F0) and the first harmonic (F1) of the membrane potential response at the grating drift frequency (Skottun et al., 1991). Hand-generated plots of receptive field structure confirmed the presence of on and off subregions in the receptive fields of simple cells classified with drifting gratings. The 17 pairs in which both cells' receptive field types were identified were assigned to one of three distinct groups, and the average correlation peak for each group is shown in Figure 5D. (Since only one pair of two simple cells [s/s] was recorded, it was not included in the analysis.) Pairs in which both cells are complex (c/c) were found to be on average more synchronized (0.46) than pairs consisting of one simple and one complex cell (s/c) (0.22). This result may be related to the relationship between synchrony and geniculate connectivity, since complex cells were more likely to

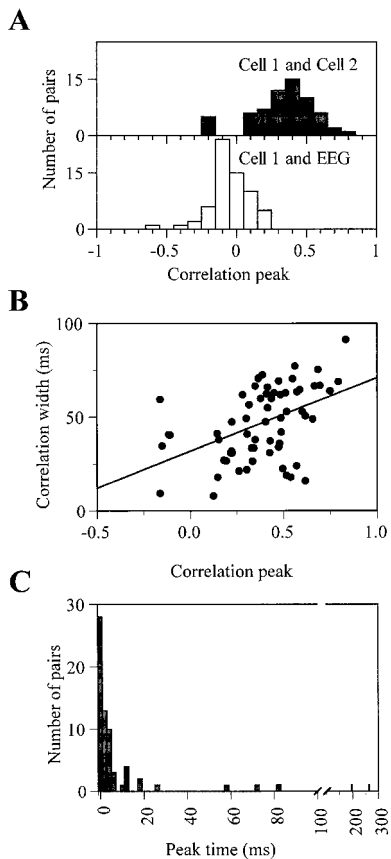


**Figure 4. Variations in Synchrony within the Sample Population**  
 (A) Histogram of the cross-correlation peaks for the 64 cell pairs in our sample (filled bars) and for one cell from each pair and the simultaneously recorded EEG (empty bars).  
 (B) The relationship between width of cross-correlation (full-width at half-height) and cross-correlation peak amplitude. Linear regression ( $r^2 = 0.21$ ;  $p < 0.0005$ , ANOVA test) shows mutual dependency of the two parameters.  
 (C) A histogram of the absolute times of the peaks of cross-correlograms for all pairs ( $N = 64$ ). All parameters were calculated from 30 s traces.

receive long latency inputs ( $>2.5$  ms) from the LGN (13/16), whereas simple cells are more likely to receive monosynaptic input.

**Spike Synchrony and Subthreshold Synchrony**

How do the subthreshold correlations in membrane potential affect the synchrony of spikes between two cells? To address this question, we first recorded the subthreshold activity from two strongly correlated cells while suppressing spikes in each cell by hyperpolarizing current injection and constructed the cross-correlogram of their membrane potentials (Figure 6A). We then applied positive current to induce firing in both cells ( $\sim 7$  spikes/s). The cross-correlogram constructed from an 85 s recording of spikes in the two cells shows a peak centered near 0 ms (Figure 6B, black curve). The shuffled correlogram (gray curve) obtained by adding 1 s to the spike times of one of the cells prior to performing the cross-correlation excludes the possibility that the peak in the correlogram arose by chance.

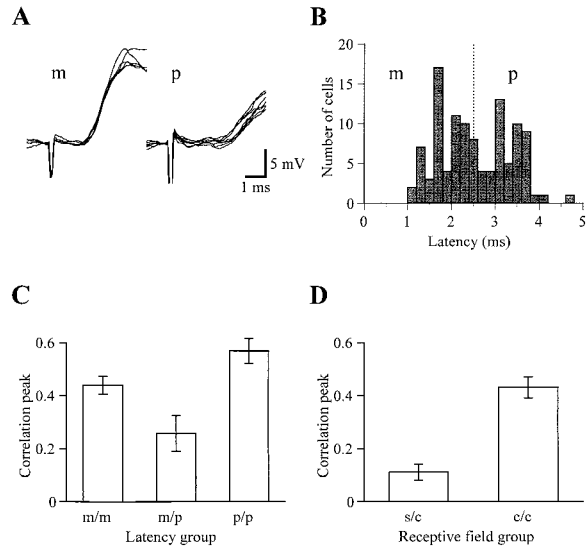


**Figure 5. Dependence of Membrane Potential Synchrony on Connectivity and Receptive Fields Types**  
 (A) Superimposed responses to electrical stimulation of the LGN. The latency to the evoked synaptic response of the first cell (“m”) is 1.8 ms, while for the second cell (“p”) the latency is 2.9 ms.  
 (B) Histogram of latencies of synaptic responses evoked in 110 cortical cells by electrical stimulation of the LGN. Cells were separated into two groups, “m” (monosynaptic) and “p” (polysynaptic), depending on whether their latencies were longer or shorter than 2.5 ms (dashed line).  
 (C) Average correlation peaks for three groups of pairs: m/m pairs in which both cells had short latencies ( $n = 20$ ); m/p pairs in which only one cell had a short latency ( $n = 17$ ); p/p pairs in which both cells had long latencies ( $n = 12$ ). The m/m and the p/p groups are significantly different from the m/p group ( $p < 0.001$ , ANOVA test, and post hoc Scheffe test with significance level of 0.05).  
 (D) Cells were characterized as either simple or complex, and the average correlation peaks were calculated for two groups of pairs, s/c ( $n = 4$ ) and c/c ( $n = 12$ ). We did not have sufficient number of s/s pairs for a significant measure of their synchrony. A significant difference was found between the two groups (t test,  $p < 0.05$ ). Error bars are  $\pm$  SEM.

To investigate the relationship between the synchronized subthreshold activity of the cells and correlated spiking, we applied spike-triggered averaging to the records used to generate the spike correlograms of Figure 6B. In Figures 6C and 6D, we used each cell’s spikes to average its own membrane potential, and in Figures 6E and 6F, we used one cell’s spikes to average the membrane potential of the second cell. In each case, the spikes (except at time 0 in Figures 6C and 6D) appear at less than their full amplitude because of the averaging. Given that the membrane potential in the two cells is strongly synchronized, it is not surprising that all four of the spike-triggered averages resemble one another, no matter which spikes serve as the trigger and which membrane potential is averaged. Spikes occur symmetrically around the peak of the membrane potential in each case. What was not expected (though see Discussion) is that the synchrony in firing is almost four times narrower than the corresponding spike-triggered averages in Figures 6E and 6F (22 ms width compared to 80 ms).

Another example of the relationship between synchrony in membrane potential and synchrony in firing

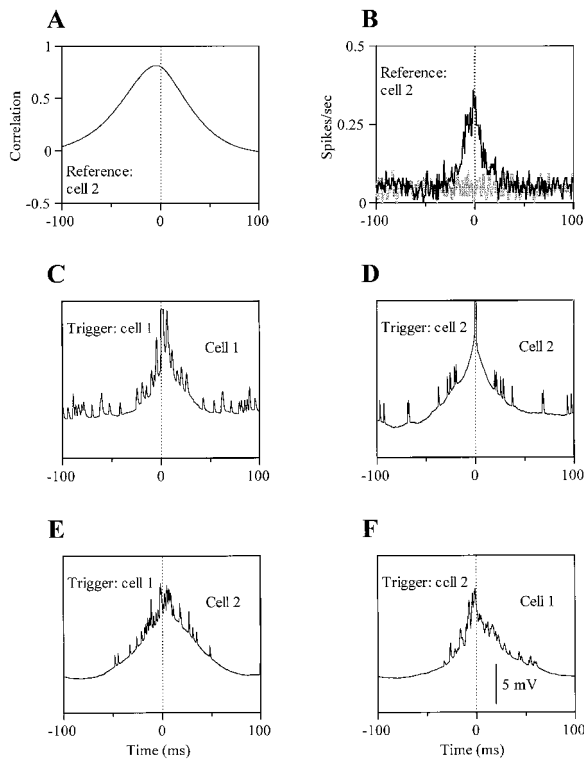


Figure 6. Correlated Firing in a Pair of Cells with Correlated Subthreshold Activity

(A) Cross-correlogram of the membrane potential in two nearby cortical cells (30 s traces). The cells were hyperpolarized with injected current to suppress action potentials.  
 (B) Black line: cross-correlogram of spikes in the two cells recorded while both cells were depolarized with injected current. The width of the correlation at half amplitude from baseline was 22 ms, and the time of the peak  $-3.5$  ms as obtained from Gaussian fit (data not shown). Gray line: cross-correlogram of spikes after spike times in one cell were shifted by 1 s.  
 (C and D) Spike-triggered average of the membrane potential of each cell, triggered from its own spikes. ([C], 30 trigger spikes; [D], 27 trigger spikes).  
 (E and F) Spike-triggered average of the membrane potential of each cell triggered by the other cell's action potentials. ([E], 22 trigger spikes; [F], 25 trigger spikes).

is shown in Figure 7. The membrane potential cross-correlogram (Figure 7A), obtained while suppressing spikes with hyperpolarizing current, was much narrower than in the previous cell. When the hyperpolarizing current was removed, synchronized firing appeared, and the cross-correlogram of spikes (Figure 7B) showed a clear peak at  $-1.0$  ms, corresponding closely to the delay in the membrane potential correlations ( $-1.5$  ms). As in the previous example, however, the width of the spike cross-correlogram (1.8 ms at half amplitude) was much smaller, in this case almost ten times smaller, than that measured for the membrane potential (17.5 ms). This extremely narrow peak in the spike correlogram with 1 ms delay might suggest that cell 2 received monosynaptic excitatory input from cell 1. The spike-triggered averages of membrane potential in the two cells suggested otherwise, however (Figures 7C–7F). The within-cell averages (Figures 7C and 7D) showed in both cases a clear rise in potential just prior the spikes. So also did

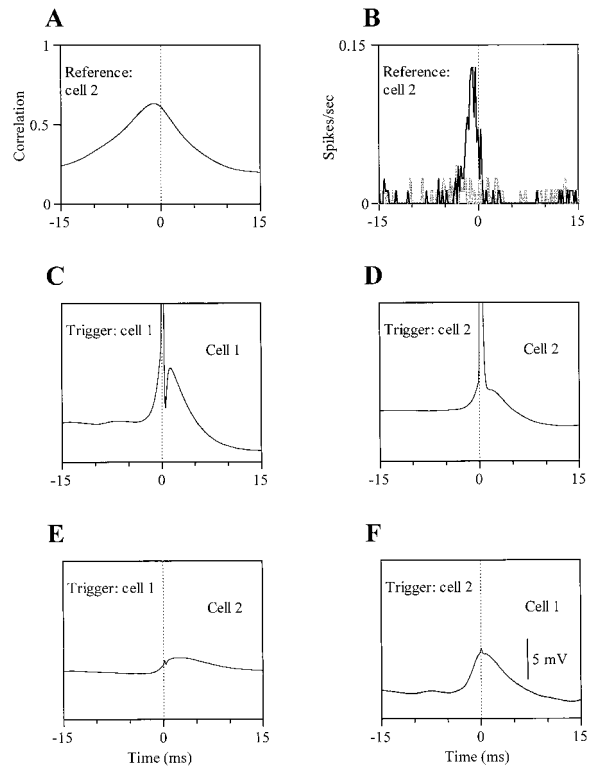


Figure 7. Correlated Firing in a Second Pair of Cells with Correlated Subthreshold Activity

(A) Cross-correlogram of the membrane potentials from a pair of cells recorded while the cells were hyperpolarized to prevent firing.  
 (B) The spike cross-correlogram for the spontaneous firing of the cells (black line) is much narrower (1.8 ms) than the cross-correlogram of membrane potentials (17.5 ms). The gray line is the cross-correlogram calculated after shifting one cell's spike times by 1 s.  
 (C and D) Spike-triggered average of the membrane potential of each cell, triggered from its own spikes ([C], 273 trigger spikes; [D], 93 trigger spikes).  
 (E and F) Spike-triggered average of the membrane potential of each cell triggered by the other cell's action potentials ([E], 273 trigger spikes; [F], 93 trigger spikes).  
 In (C)–(F), only records containing no spikes other than the trigger spikes were included in the averages.

the across-cell averages (Figures 7E and 7F), with the trigger spikes occurring either on the rising phase of the potential (Figure 7E) or at the peak (Figure 7F). (The small potentials at time 0 in the across-cell averages are spike artifacts of electrical coupling between the two electrodes.) Since the potentials start before the trigger spike, and there is no clear inflection after the trigger spike, it is unlikely that these correlated potentials, or the correlated spikes in Figure 7B, are generated by synaptic input between the two cells, but instead arise from common input from other cells.

#### Effect of Visual Stimulation on Correlations

Our results so far indicate that the subthreshold activity of neighboring complex cells in V1 is highly synchronized in the absence of visual stimulation. To understand how the correlation between cells is affected by visual stimulation, we recorded from three pairs of complex cells while presenting drifting gratings of different orientations. The pair in Figure 8 was typical of our sample

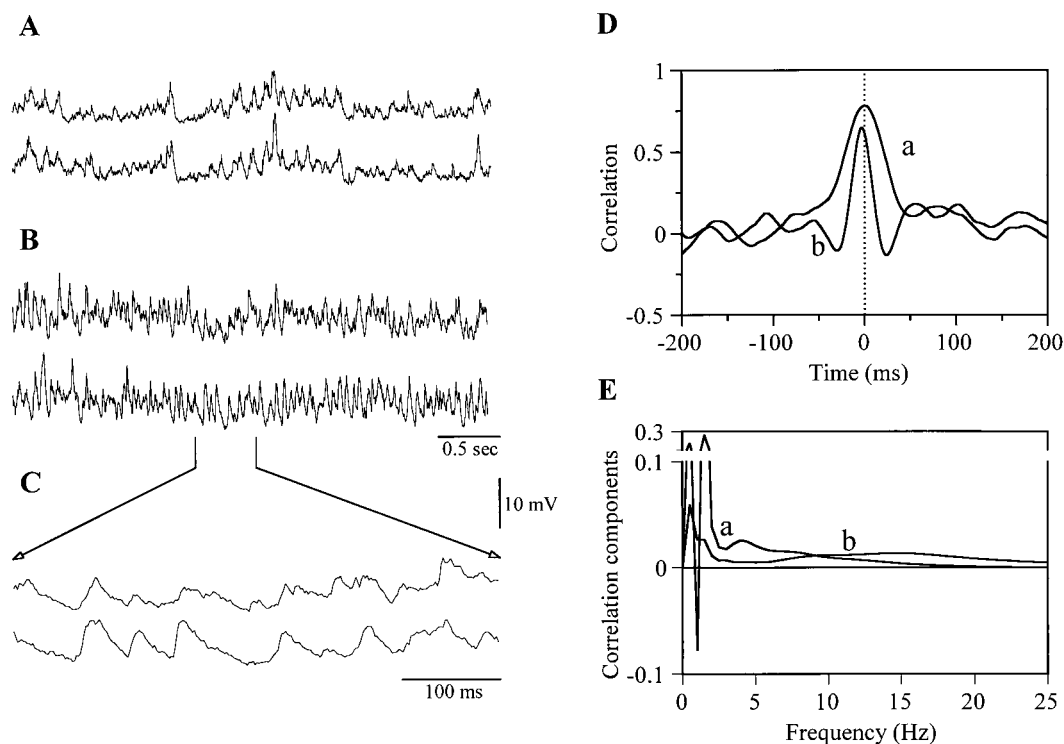


Figure 8. The Effect of Visual Stimulation on Membrane Potential Synchrony between Neighboring Complex Cells

(A) Simultaneous intracellular records of spontaneous activity from a pair of highly synchronized complex cells.  
 (B) Traces recorded from the same cells during the presentation of sinusoidal drifting grating (2 Hz, 0.54 cycles/degree, 64% contrast).  
 (C) Expanded 0.5 s epoch from (B).  
 (D) Cross-correlograms for traces in (A) (curve a) and (B) (curve b). During visual stimulation, the peak in the correlogram decreases slightly and at the same time narrows significantly.  
 (E) Individual frequency components contribute differently to spontaneous (a) and visually evoked (b) synchrony. To obtain these curves, the traces from each cell were first digitally high-pass filtered (Butterworth, fourth order) at 50 different frequencies between 0 and 25 Hz. The cross-correlation (normalized by the standard deviations of the unfiltered traces) was then calculated for each filter frequency. The value of each of the 50 resulting correlograms was measured at the time of the peak in (D) (1 ms for spontaneous activity and -2.5 ms for visually evoked activity). These values were differentiated with respect to filter cutoff frequency and plotted in (E).

in showing slow correlated fluctuations in membrane potential in the absence of visual stimulation (Figures 8A and 8D, curve a). When a 2 Hz drifting grating near the preferred orientations for the two cells was introduced (Figures 8B and 8C), both cells responded with a steady depolarization (upper cell, 4.3 mV; lower cell, 3.0 mV) and an increase in the small amplitude, high-frequency components of the traces. At the same time, the slow fluctuations characteristic of the spontaneous activity were largely suppressed. These changes in the dominant frequency components of the traces are reflected in the 2.6-fold reduction in the width of the correlogram (Figure 8D, curve b). Nevertheless, the two cells are still highly correlated, with only a modest (14%) reduction in the peak amplitude of the correlogram compared to the spontaneous records.

To determine which frequency components of the responses contributed to synchrony, we high-pass filtered the traces at 50 different cutoff frequencies between 0 and 25 Hz and calculated the cross-correlation between the filtered signals. The relationship between cutoff frequency and correlation peak was then differentiated with respect to frequency. For example, the difference in the correlation strength between traces high-pass

filtered at 5 and 5.5 Hz will give an indication of the contribution of the 5–5.5 Hz frequency band to the overall correlation of the signals. This number can be either positive or negative. The resulting curves are shown in Figure 8E for the spontaneous and stimulus-evoked responses from Figures 8A and 8B. During spontaneous activity, low frequencies (0.5–3 Hz) are the major contributors to synchrony, with a secondary contribution at 4–10 Hz. During visual stimulation, the contribution from the very low-frequency components is decreased significantly, and the secondary peak shifts to between 10 and 20 Hz. Visual stimulation clearly changes the temporal characteristics of the synaptic events that contribute to synchronization.

The effect of changing stimulus orientation on the correlation between two complex cells is illustrated in Figures 9A–9E. The orientation tuning curves (Figure 9A) indicate that the preferred orientations of the cells differed by 30°. Gratings of different orientations were then presented for 30 s at each of ten orientations. The dependence of the peak amplitude and width of the correlograms on orientation is shown in Figures 9B and 9C. Correlations became stronger and up to 3-fold narrower than the spontaneous level (horizontal lines) when

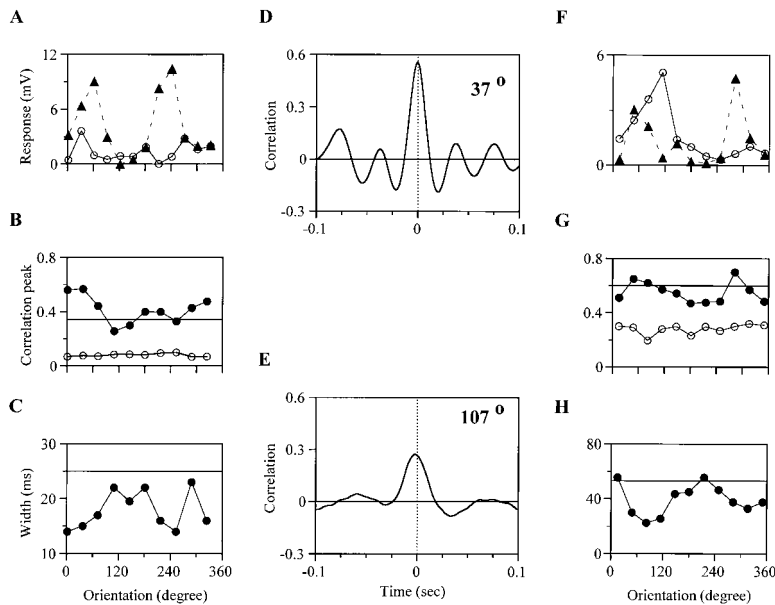


Figure 9. The Effect of Stimulus Orientation on Membrane Potential Synchrony in Two Pairs of Complex Cells

(A) Orientation tuning curves of the mean change in membrane potential (relative to rest) in two simultaneously recorded complex cells. Tuning curves were measured from responses to 4 s presentations of sinusoidal drifting gratings (2 Hz, 0.54 cycles/degree, 64% contrast) at 12 different orientations.

(B) Closed symbols: peak amplitude of the cross-correlation calculated for 30 s responses to gratings at ten different orientations. Open symbols: peak amplitude of the cross-correlation calculated after the record from one cell was shifted in time by one stimulus period (0.5 s). The horizontal line represents the correlation peak measured during spontaneous activity.

(C) Width of the peaks of the cross-correlogram as a function of stimulus orientation. The horizontal line represents the width of the cross-correlogram peak calculated from the spontaneous activity.

(D and E) Sample cross-correlograms for two different stimulus orientations.

(F–H) Same as (A)–(C) for a second pair of complex cells.

both neurons responded strongly to the stimulus, and weaker when neither cell was responding. Sample correlograms for two different orientations are shown in Figures 9D and 9E. Figure 9D shows some oscillatory activity at a frequency of 25 Hz, but oscillations of this type were relatively rare in our sample, having been observed in only four pairs.

Results from a second pair of complex cells are shown in Figures 9F–9H. As for the previous pair, the correlation peaks are slightly higher than the spontaneous level for stimuli that evoked activity in both cells, and lower for orientations at which neither cell responded. The widths follow opposite trends. In a third pair of neurons (data not shown), we found no clear effect of stimulus orientation on the degree of correlation.

One concern that arises from Figure 9 is that the stimulus might affect the correlation between the two cells by evoking membrane potential changes in each cell that are phase locked to the stimulus cycle. These signals in the two cells would in turn be phase locked to each other and give rise to orientation dependent changes in synchrony. To test for this possibility, we measured the correlation between the two cells after shifting the potential record of one cell in time by one stimulus cycle. The correlation in this case drops significantly and does not vary with orientation. The changes in synchrony, then, are stimulus related, but not stimulus locked.

## Discussion

### Origins of the Slow Fluctuations of Membrane Potential

In our recordings, the largest correlations in membrane potential occurred between cells that showed large and slow spontaneous fluctuations in their membrane potentials (Figures 3A–3D). These fluctuations are highly reminiscent of bimodal fluctuations in membrane potential

described in neostriatal (Wilson and Kawaguchi, 1996) and corticostriatal neurons (Wilson et al., 1983). More recently, similar potentials have been observed in motor cortex (Contreras et al., 1996), and hints of these fluctuations are visible in records from V1 neurons published by Douglas et al. (1991 [see their Figures 5, 8, 14, and 17]). Unlike the corticostriatal neurons, however, the neurons in our study did not always show two distinct membrane potential states and appeared to be more irregular in duration (Ferster and Carandini, 1996).

Some previous experiments suggested that these large and slow spontaneous events occur simultaneously in a large number of neurons within a cortical column. Ferster and Carandini (1996) showed that in the visual cortex, spontaneous intracellular fluctuations in membrane potential are highly correlated with the local field potential. The local field potentials are in turn correlated with spikes in individual neurons and with optically detected spontaneous neuronal events that cover several millimeters of the cortical surface (Arieli et al., 1995). While these experiments suggest that nearby neurons are highly correlated, the correlation appears not to extend far beyond a small region of cortex: we found only weak correlations between intracellular membrane potential and the EEG recorded some distance away. On rare occasions, stronger correlations were observed, but these were limited to periods during which large numbers of spindles were present in the EEG.

Amzica and Steriade (1995b) have observed, in contrast to our results, that low-frequency fluctuations in membrane potential can be strongly correlated over large regions of the cortex, and even across hemispheres (Contreras and Steriade, 1995). There are important differences between their results and ours, however. The frequencies of the underlying potentials that contribute to the correlations in their records are far slower than reported here. Consequently, the widths of the correlations that Amzica and Steriade and Contreras

and Steriade reported are up to ten times wider than those we have observed. Second, the correlograms presented in these papers show strong periodicity at low frequencies ( $<1$  Hz), a feature that was not present in our records. Third, Contreras and Steriade (1997) have reported that long-range, very low-frequency correlations are strengthened by placing the animal in a deeper state of anesthesia, whereas we made an attempt to keep the animals under light surgical anesthesia. So while the two sets of observations may share similar mechanisms, there is a clear difference in the spatial extent and temporal dynamics of correlations in our experiments and in those of Steriade and his colleagues.

These results raise the question of whether slow fluctuations in membrane potential, and therefore strong correlations among neurons, perhaps do not occur in the awake animal, but are an artifact of anesthesia. Several pieces of evidence speak against this possibility. (1) The correlation between intracellular potentials and the EEG is weak. (2) The membrane potentials that are the basis for much of the correlation between cells are not dependent on the choice of anesthetic agent. Membrane potentials similar to those we have observed have been reported in neocortical cells using pentothal (Douglas et al., 1991; the current study), ketamine/xylazine (Pare et al., 1998), Saffan (Douglas et al., 1991), and urethane (Wilson and Kawaguchi, 1996). In addition, we have seen strong correlations using urethane and halothane (in collaboration with Drs. Amos Arieli and Amiram Grinvald). (3) The correlations are not limited to the lowest frequency components of the intracellular signals that are most strongly affected by anesthetic (Figures 1E and 1F). (4) Wilson and Groves (1981) recorded from awake rats and observed the fluctuations without any anesthetic at all. (5) Arieli has found (Arieli et al., 1996, *Soc. Neurosci.*, abstract) that events in the local field potential recorded from the motor cortex, which in visual cortex are correlated with large fluctuations in the membrane potential, are related to reaction times in awake, behaving monkey performing a motor task. Nevertheless, the question remains as to whether the strong membrane potential correlations that occur in anesthetized animals also occur in the awake animal and, if correlations exist in awake animals, whether they have similar properties and underlying mechanisms to those that we have observed here.

### Mechanisms Underlying Synchrony

What is the origin of the spontaneous synchronized activity that we observe? One possibility is that the two cells and others in the local area are all driven by a common input of remote origin. It has been suggested, for example, that  $\gamma$  frequency oscillations in the visual cortex are generated remotely in the LGN (Ghose and Freeman, 1992) or retina (Neuenschwander and Singer, 1996; Castelo-Branco et al., 1998). Alternatively, synchronized activity could be organized locally through recurrent synaptic interactions. Silva et al. (1991) have shown in vitro that spontaneous or electrically evoked activity in layer 5 can drive other layers of the cortex when neuronal excitability is enhanced pharmacologically.

Whatever initiates the activity that we observe, the propagation of the activity is likely to be supported by the intralaminar and lateral intracortical connections within the cortex. These connections are densest and project for long distances in the supra- and infragranular layers (Gilbert and Kelly, 1975; Gilbert and Wiesel, 1989). A role for lateral connections within the cortex in synchronizing activity among cells is supported by Amzica and Steriade (1995a). When they inactivated the cortex between two neurons separated by 15 mm with lidocaine injections, the correlation between the neurons was greatly reduced. While our neurons were much closer together ( $<500$   $\mu\text{m}$ ), it is possible that similar mechanisms are at work.

The synchrony between cells present during visual stimulation may arise from the same mechanisms as synchrony in spontaneous activity. The drifting gratings that we employed generate a massive stimulus-locked synchrony in LGN relay cells and cortical simple cells. This phase locking, however, is not directly responsible for the synchrony among complex cells (Figure 9). Thus, the synchrony among complex cells in the presence of visual stimulation likely arises from local mechanisms, perhaps through the same lateral connections mentioned above. But if spontaneous and visually evoked synchrony arise from the same circuitry, what causes the narrowing of the correlograms that occurs in cells that are responding vigorously to a stimulus (Figures 8 and 9)? One possibility might be related to visually evoked decreases in neuronal input resistance (Borg-Graham et al., 1996, 1998; Hirsch et al., 1998). A decrease in input resistance would result in a decrease in time constant, which could filter out low-frequency synaptic events and lead to a narrowing of the peak in the cross-correlogram.

### Synchrony among Subpopulations of Cortical Neurons

In the absence of visual stimulation, some cortical neurons are highly correlated with one another while others are less so. What cell properties determine whether a group of cells will correlate with one another? Synchrony is strongly related to two properties that are dependent on a neuron's position within the visual pathway, connectivity, and receptive field type. Cells with polysynaptic inputs from the LGN tend to synchronize with each other, as do cells with monosynaptic input, but cells tend not to synchronize across groups. Similarly, complex cells are more strongly synchronized with other complex cells and less so with other simple cells. At the very least, these results suggest that in the absence of visual stimulation, the cortex is loosely divided into two functionally distinct circuits, each with its own internal synchrony. Given that the connectivity and receptive field types of neurons vary with cortical layers (Gilbert, 1977; Ferster and Lindstrom, 1983, 1985; Hata et al., 1991), the distinct circuits might correspond roughly to different cortical layers or groups of layers.

Visual stimulation superimposes on this horizontal pattern of synchrony a columnar pattern. The optical recordings of Arieli and colleagues (1995, 1996) indicate that the synchrony across the surface of the cortex is

relatively undifferentiated in the absence of a stimulus. In the presence of a visual stimulus (Figure 9), however, the degree of synchronization between cells increased or decreased depending on whether the cells were simultaneously active or not. At the same time, the width of correlation is also strongly modulated. This surely means that cells within different orientation columns will exhibit different degrees of synchrony depending on the visual stimulus. This columnar pattern could interact in a complex way with the ongoing activity, since neurons that are not responding to the stimulus, though less strongly correlated than in the absence of a stimulus, retain a significant degree of synchrony (Figure 9). One might have speculated that the visual stimulus, acting through lateral inhibitory connections, would completely disrupt the broad, horizontally oriented pattern of spontaneous synchrony and replace it with a purely columnar pattern. Instead, it appears that the horizontal pattern remains intact and is reorganized only within the columns of cells responding to the stimulus.

#### Membrane Potential Synchrony and Spike Synchrony

What events are occurring in the membrane potentials of two cells to give rise to the synchronized spikes that are so often observed extracellularly? One possibility is that the cells receive occasional brief bursts of synchronous suprathreshold synaptic activity. In this scenario, when the cells are not spiking the synaptic inputs would be largely uncorrelated. Our results suggest just the opposite: that correlation of the synaptic inputs occurs almost continuously.

What determines the exact relationship between the shape of the correlogram for subthreshold potentials on the one hand and the spike correlogram on the other? In our data, the spike correlations are invariably much narrower than the subthreshold correlations, by a factor of up to 10 (Figures 6 and 7). It is not difficult to arrive at a possible mechanism for this difference in widths. One can take the extreme case in which the membrane potentials of two cells are identical, but slowly varying, making the correlogram of the membrane potentials very broad. Assuming that threshold was identical in the two cells, as the potential in the two cells reached threshold, the two cells would fire simultaneously, leading to a very narrow spike correlogram. The problem with this scenario is its extreme simplicity. Slight changes in threshold, DC offset, or amplitude of the membrane potential fluctuations in one cell would change the cell's spike times and severely distort or shift the spike correlogram, without changing the membrane potential correlogram at all. Given that the fluctuations in the two cells are never completely identical, it is striking that the spike correlograms are as narrow as they are and that they have very similar temporal offsets to the membrane potential correlograms. This would suggest that even in the presence of large, slow fluctuations in the membrane potential, it is the higher-frequency components that play the decisive role in triggering spikes (Reyes and Fetz, 1993a, 1993b; Mainen and Sejnowski, 1995).

Spike correlation is often used as an indication of connectivity. Wide spike correlograms (15–80 ms) are

thought to arise from nonspecific common synaptic inputs (Kruger and Aiple, 1988; Eckhorn et al., 1993). Some neurons, for example, could make monosynaptic connections with one cell in a pair, and polysynaptic connections with the other cell, broadening the correlogram and shifting its peak away from zero. Narrower correlations with delays centered near zero likely represent more specific common input, such as a monosynaptic input to each cell from a third group of cells (Toyama et al., 1981a, 1981b; Ts'o et al., 1986). Narrow spike correlations with delays displaced from zero have been interpreted as reflecting monosynaptic connections from one cell to another (Toyama et al., 1981a, 1981b; Ts'o et al., 1986; Alonso et al., 1996). Our results suggest, however, that these interpretations need to be made cautiously. The spike correlation between the cells in Figure 7, for example, is extremely narrow and is displaced from time zero, and yet the intracellular records suggest that any monosynaptic connections between these neurons are weak at best.

#### Functional Significance of Subthreshold Synchronization

Synchronization among nearby and widely separated neurons (Gray et al., 1989; Gray and Singer, 1989; Engel et al., 1991a, 1991c) has been postulated to contribute to higher perceptual processes such as feature binding (Singer and Gray, 1995). In an analogous proposal, synchronous activity in the motor cortex (Murthy and Fetz, 1996; Riehle et al., 1997; Lee et al., 1998) might be integral to motor processing. Synchrony has also been suggested as a mechanism of lower level coding. In the visual system, synchronous spikes in nearby cells act as a kind of virtual neuron with its own small receptive field made up of the overlapping regions of the two cell's receptive fields (Ghose et al., 1994; Meister et al., 1995; Alonso et al., 1996). The membrane potential synchrony that we have observed could contribute to synchronized firing observed in many of these studies.

On the other hand, strong synchrony among large populations of neurons could interfere with one aspect of information coding. One of the fundamental questions relevant to neuronal coding is whether the responses of different neurons to a single stimulus are independent or not. That is, is the trial-to-trial variability of the response in one neuron related to the variability in nearby neurons? This question is critical to population coding. Response variability is usually associated with noise, and a common assumption is that by averaging the signals from many neurons, the brain reduces noise and improves the detection of weak stimuli (Zohary et al., 1994; Britten and Newsome, 1998; Lee et al., 1998). But averaging mechanisms are effective only if the noise in different neurons is independent, which our results suggest is not the case. Even during a visual stimulus, large membrane potential variations that are not locked to the stimulus itself occur synchronously in two neurons. Assuming that this activity constitutes noise and not signal, the synchrony must surely reduce the efficacy of averaging in improving the resolution or detectability of neuronal signals.

There are other, more subtle possible functions for the

correlation of low-frequency signals in cortical neurons. Results from Lampl and Yarom (1993) in the inferior olive have suggested that asynchronous synaptic inputs, when superimposed on synchronous slow fluctuations, can result in nearly synchronous spikes (Reyes and Fetz, 1993b). One can speculate that in cortex, slow fluctuations of local origin serve to synchronize the output of neurons that receive visual inputs that are dispersed in time by different conduction times (such as X and Y cells) or simply by random trial to trial variations in visual latency. Alternatively, the synchronous slow fluctuations in membrane potential could serve to synchronize changes in the excitability of specific groups of cells while the fine pattern of spikes is then determined by asynchronous synaptic inputs (Stern et al., 1998). At present, however, the exact function of this relatively new phenomenon remains to be determined.

#### Experimental Procedures

Recordings were obtained from paralyzed, anesthetized, adult cats using methods similar to Chung and Ferster (1998).

#### Electrophysiology

##### Intracellular Recordings

Intracellular records were obtained with conventional sharp microelectrodes pulled from standard borosilicate glass and filled with 2 M potassium acetate (resistance 40–90 M $\Omega$ ). Two electrodes were placed on the cortical surface with their tips less than 500  $\mu$ m apart and angled approximately 10°–15° to the vertical axis so that they would approach each other as they were advanced into the cortex. The exposed cortex was then covered with warm agar (3% in 0.9% saline) to lessen respiratory and cardiovascular movements and prevent the cortex from drying. Electrodes were advanced with a stepping microdrive (Transvertex) and a hydraulic microdrive (Newport Corp., CA). The electrodes were advanced alternately, so the depth difference was kept as small as possible. From the geometry of the electrode placement, the cells recorded in a pair were never more than 500  $\mu$ m apart horizontally. Membrane potentials were recorded with an Axoclamp-2A amplifier (Axon Instruments, Foster City, CA) in a bridge mode. Membrane potentials were low-pass filtered at 10 kHz prior to digitization at 20 kHz. The EEG was band-pass filtered (1–100 Hz) prior to digitization at 400 Hz.

##### Electrical Stimulation of the LGN

A lacquer-coated tungsten electrode was placed stereotaxically in the LGN ipsilateral to the cortical recording site, and its position adjusted so that the receptive fields of units recorded at its tip were within 2°–4° of the area centralis. Stimuli consisted of 200  $\mu$ s, 1 mA cathodal pulses.

#### Visual Stimulation

Receptive fields were first characterized by hand with bars of light projected onto a tangent screen. During data collection, drifting sinusoidal gratings were presented on an oscilloscope screen (Tektronix, Beaverton, OR) driven by Picasso image synthesizer (Innisfree, Cambridge, MA). The average screen luminance was 20 cd/m<sup>2</sup>.

#### Cross-Correlation Analysis

The signals were first digitally high-pass filtered (1-Hz Butterworth, second order) to prevent the correlograms from registering slow shifts in DC potentials. The extent of correlation between the signals was calculated according to the following equation:

$$h(\tau) = \frac{\sum_{i=-T}^T (x_i - \bar{x})(y_{i+\tau} - \bar{y})}{\sqrt{\sum_{i=-T}^T (x_i - \bar{x})^2 \sum_{i=-T}^T (y_i - \bar{y})^2}} \quad (1)$$

where  $x$  and  $y$  are signals from the two neurons,  $2T + 1$  is the number of samples in each signal and spanned either 1 s or 30 s (see text), and  $\bar{x}$  and  $\bar{y}$  are the means of the signals. The denominator is the product of the standard deviations of the two signals and therefore normalizes the cross-correlation. Thus,  $h(0)$  for two input signals that are identical (or are scaled versions of one another) will have a value of 1.

Spike correlograms (histograms of the latencies of the spikes in one cell measured relative to spikes of the second cell in the pair) were calculated with a bin width of 1 ms. Histograms were normalized such that their integrals are equal to one. To obtain the frequency (in Hz) of coincident events at various delays, the counts values were divided by the total time of data collection.

#### Acknowledgments

We are grateful to Sooyoung Chung, Deda Gillespie, Matteo Carandini, and Nelson Spruston for comments on the manuscript. This work was supported by a grant EY04726 from the National Eye Institute.

Received May 5, 1998; revised January 19, 1999.

#### References

- Alonso, J.M., Usrey, W.M., and Reid, R.C. (1996). Precisely correlated firing in cells of the lateral geniculate nucleus. *Nature* **383**, 815–819.
- Amzica, F., and Steriade, M. (1995a). Disconnection of intracortical synaptic linkages disrupts synchronization of a slow oscillation. *J. Neurosci.* **15**, 4658–4677.
- Amzica, F., and Steriade, M. (1995b). Short- and long-range neuronal synchronization of the slow (<1 Hz) cortical oscillation. *J. Neurophysiol.* **73**, 20–38.
- Arieli, A., Shoham, D., Hildesheim, R., and Grinvald, A. (1995). Coherent spatiotemporal patterns of ongoing activity revealed by real-time optical imaging coupled with single-unit recording in the cat visual cortex. *J. Neurophysiol.* **73**, 2072–2093.
- Arieli, A., Sterkin, A., Grinvald, A., and Aertsen, A. (1996). Dynamics of ongoing activity: explanation of the large variability in evoked cortical responses. *Science* **273**, 1868–1871.
- Borg-Graham, L., Monier, C., and Fregnac, Y. (1996). Voltage-clamp measurement of visually-evoked conductances with whole-cell patch recordings in primary visual cortex. *J. Physiol. Paris* **90**, 185–188.
- Borg-Graham, L.J., Monier, C., and Fregnac, Y. (1998). Visual input evokes transient and strong shunting inhibition in visual cortical neurons. *Nature* **393**, 369–373.
- Britten, K.H., and Newsome, W.T. (1998). Tuning bandwidths for near-threshold stimuli in area MT. *J. Neurophysiol.* **80**, 762–770.
- Castelo-Branco, M., Neuenschwander, S., and Singer, W. (1998). Synchronization of visual responses between the cortex, lateral geniculate nucleus, and retina in the anesthetized Cat. *J. Neurosci.* **18**, 6395–6410.
- Chung, S., and Ferster, D. (1998). Strength and orientation tuning of the thalamic input to simple cells revealed by electrically evoked cortical suppression. *Neuron* **20**, 1177–1189.
- Contreras, D., and Steriade, M. (1995). Cellular basis of EEG slow rhythms: a study of dynamic corticothalamic relationships. *J. Neurosci.* **15**, 604–622.
- Contreras, D., and Steriade, M. (1997). State-dependent fluctuations of low-frequency rhythms in corticothalamic networks. *Neuroscience* **76**, 25–38.
- Contreras, D., Timofeev, I., and Steriade, M. (1996). Mechanisms of long-lasting hyperpolarizations underlying slow sleep oscillations in cat corticothalamic networks. *J. Physiol. (Lond)* **494**, 251–264.
- deCharms, R.C., and Merzenich, M.M. (1996). Primary cortical representation of sounds by the coordination of action-potential timing. *Nature* **381**, 610–613.

- Douglas, R.J., Martin, K.A., and Whitteridge, D. (1991). An intracellular analysis of the visual responses of neurones in cat visual cortex. *J. Physiol. (Lond)* *440*, 659–696.
- Eckhorn, R., Krause, F., and Nelson, J.I. (1993). The RF-cinematogram. A cross-correlation technique for mapping several visual receptive fields at once. *Biol. Cybern.* *69*, 37–55.
- Engel, A.K., Konig, P., Kreiter, A.K., and Singer, W. (1991a). Interhemispheric synchronization of oscillatory neuronal responses in cat visual cortex. *Science* *252*, 1177–1179.
- Engel, A.K., Konig, P., and Singer, W. (1991b). Direct physiological evidence for scene segmentation by temporal coding. *Proc. Natl. Acad. Sci. USA* *88*, 9136–9140.
- Engel, A.K., Kreiter, A.K., Konig, P., and Singer, W. (1991c). Synchronization of oscillatory neuronal responses between striate and extrastriate visual cortical areas of the cat. *Proc. Natl. Acad. Sci. USA* *88*, 6048–6052.
- Ferster, D., and Carandini, M. (1996). Spontaneous fluctuations in membrane potential of complex cells in visual cortex, *Soc. Neurosci. Abstr.* *22*, 490.
- Ferster, D., and Lindstrom, S. (1983). An intracellular analysis of geniculate-cortical connectivity in area 17 of the cat. *J. Physiol. (Lond)* *342*, 181–215.
- Ferster, D., and Lindstrom, S. (1985). Synaptic excitation of neurones in area 17 of the cat by intracortical axon collaterals of corticogeniculate cells. *J. Physiol. (Lond)* *367*, 233–252.
- Freiwald, W.A., Kreiter, A.K., and Singer, W. (1995). Stimulus dependent intercolumnar synchronization of single unit responses in cat area 17. *Neuroreport* *6*, 2348–2352.
- Ghose, G.M., and Freeman, R.D. (1992). Oscillatory discharge in the visual system: does it have a functional role? *J. Neurophysiol.* *68*, 1558–1574.
- Ghose, G.M., Ohzawa, I., and Freeman, R.D. (1994). Receptive-field maps of correlated discharge between pairs of neurons in the cat's visual cortex. *J. Neurophysiol.* *71*, 330–346.
- Gilbert, C.D. (1977). Laminar differences in receptive field properties of cells in cat primary visual cortex. *J. Physiol. (Lond)* *268*, 391–421.
- Gilbert, C.D., and Kelly, J.P. (1975). The projections of cells in different layers of the cat's visual cortex. *J. Comp. Neurol.* *163*, 81–105.
- Gilbert, C.D., and Wiesel, T.N. (1989). Columnar specificity of intrinsic horizontal and corticocortical connections in cat visual cortex. *J. Neurosci.* *9*, 2432–2442.
- Gray, C.M., and Singer, W. (1989). Stimulus-specific neuronal oscillations in orientation columns of cat visual cortex. *Proc. Natl. Acad. Sci. USA* *86*, 1698–1702.
- Gray, C.M., Konig, P., Engel, A.K., and Singer, W. (1989). Oscillatory responses in cat visual cortex exhibit inter-columnar synchronization which reflects global stimulus properties. *Nature* *338*, 334–337.
- Hata, Y., Tsumoto, T., Sato, H., and Tamura, H. (1991). Horizontal interactions between visual cortical neurones studied by cross-correlation analysis in the cat. *J. Physiol. (Lond)* *441*, 593–614.
- Hirsch, J.A., Alonso, J.M., Reid, R.C., and Martinez, L.M. (1998). Synaptic integration in striate cortical simple cells. *J. Neurosci.* *18*, 9517–9528.
- Kruger, J., and Aiple, F. (1988). Multimicroelectrode investigation of monkey striate cortex: spike train correlations in the infragranular layers. *J. Neurophysiol.* *60*, 798–828.
- Lamp, I., and Yarom, Y. (1993). Subthreshold oscillations of the membrane potential: a functional synchronizing and timing device. *J. Neurophysiol.* *70*, 2181–2186.
- Lee, D., Port, N.L., Kruse, W., and Georgopoulos, A.P. (1998). Variability and correlated noise in the discharge of neurons in motor and parietal areas of the primate cortex. *J. Neurosci.* *18*, 1161–1170.
- Mainen, Z.F., and Sejnowski, T.J. (1995). Reliability of spike timing in neocortical neurons. *Science* *268*, 1503–1506.
- Martin, K.A., and Whitteridge, D. (1984a). Form, function and intracortical projections of spiny neurones in the striate visual cortex of the cat. *J. Physiol. (Lond)* *353*, 463–504.
- Martin, K.A., and Whitteridge, D. (1984b). The relationship of receptive field properties to the dendritic shape of neurones in the cat striate cortex. *J. Physiol. (Lond)* *356*, 291–302.
- Meister, M. (1996). Multineuronal codes in retinal signaling. *Proc. Natl. Acad. Sci. USA* *93*, 609–614.
- Meister, M., Lagnado, L., and Baylor, D.A. (1995). Concerted signaling by retinal ganglion cells. *Science* *270*, 1207–1210.
- Murthy, V.N., and Fetz, E.E. (1996). Oscillatory activity in sensorimotor cortex of awake monkeys: synchronization of local field potentials and relation to behavior. *J. Neurophysiol.* *76*, 3949–3967.
- Neuenschwander, S., and Singer, W. (1996). Long-range synchronization of oscillatory light responses in the cat retina and lateral geniculate nucleus. *Nature* *379*, 728–732.
- Nicolelis, M.A., Baccala, L.A., Lin, R.C., and Chapin, J.K. (1995). Sensorimotor encoding by synchronous neural ensemble activity at multiple levels of the somatosensory system. *Science* *268*, 1353–1358.
- Nowak, L.G., Munk, M.H., Nelson, J.I., James, A.C., and Bullier, J. (1995). Structural basis of cortical synchronization. I. Three types of interhemispheric coupling. *J. Neurophysiol.* *74*, 2379–2400.
- Pare, D., Shink, E., Gaudreau, H., Destexhe, A., and Lang, E.J. (1998). Impact of spontaneous synaptic activity on the resting properties of cat neocortical pyramidal neurons in vivo. *J. Neurophysiol.* *79*, 1450–1460.
- Plenz, D., and Kitai, S.T. (1998). Up and down states in striatal medium spiny neurons simultaneously recorded with spontaneous activity in fast-spiking interneurons studied in cortex-striatum-substantia nigra organotypic cultures. *J. Neurosci.* *18*, 266–283.
- Reyes, A.D., and Fetz, E.E. (1993a). Effects of transient depolarizing potentials on the firing rate of cat neocortical neurons. *J. Neurophysiol.* *69*, 1673–1683.
- Reyes, A.D., and Fetz, E.E. (1993b). Two modes of interspike interval shortening by brief transient depolarizations in cat neocortical neurons. *J. Neurophysiol.* *69*, 1661–1672.
- Riehle, A., Grun, S., Diesmann, M., and Aertsen, A. (1997). Spike synchronization and rate modulation differentially involved in motor cortical function. *Science* *278*, 1950–1953.
- Silva, L.R., Amitai, Y., and Connors, B.W. (1991). Intrinsic oscillations of neocortex generated by layer 5 pyramidal neurons. *Science* *251*, 432–435.
- Singer, W., and Gray, C.M. (1995). Visual feature integration and the temporal correlation hypothesis. *Annu. Rev. Neurosci.* *18*, 555–586.
- Skottun, B.C., De Valois, R.L., Grosf, D.H., Movshon, J.A., Albrecht, D.G., and Bonds, A.B. (1991). Classifying simple and complex cells on the basis of response modulation. *Vision Res.* *31*, 1079–1086.
- Steriade, M., Nunez, A., and Amzica, F. (1993). A novel slow (<1 Hz) oscillation of neocortical neurons in vivo: depolarizing and hyperpolarizing components. *J. Neurosci.* *13*, 3252–3265.
- Stern, E.A., Jaeger, D., and Wilson, C.J. (1998). Membrane potential synchrony of simultaneously recorded striatal spiny neurons in vivo. *Nature* *394*, 475–478.
- Stevens, C.F., and Zador, A.M. (1998). Input synchrony and the irregular firing of cortical neurons. *Nat. Neurosci.* *1*, 210–217.
- Toyama, K., Kimura, M., and Tanaka, K. (1981a). Cross-correlation analysis of interneuronal connectivity in cat visual cortex. *J. Neurophysiol.* *46*, 191–201.
- Toyama, K., Kimura, M., and Tanaka, K. (1981b). Organization of cat visual cortex as investigated by cross-correlation technique. *J. Neurophysiol.* *46*, 202–214.
- Ts'o, D.Y., Gilbert, C.D., and Wiesel, T.N. (1986). Relationships between horizontal interactions and functional architecture in cat striate cortex as revealed by cross-correlation analysis. *J. Neurosci.* *6*, 1160–1170.
- Vaadia, E., Haalman, I., Abeles, M., Bergman, H., Prut, Y., Slovin, H., and Aertsen, A. (1995). Dynamics of neuronal interactions in monkey cortex in relation to behavioural events. *Nature* *373*, 515–518.
- Wilson, C.J., and Groves, P.M. (1981). Spontaneous firing patterns of identified spiny neurons in the rat neostriatum. *Brain Res.* *220*, 67–80.

Wilson, C.J., and Kawaguchi, Y. (1996). The origins of two-state spontaneous membrane potential fluctuations of neostriatal spiny neurons. *J. Neurosci.* *16*, 2397–2410.

Wilson, C.J., Chang, H.T., and Kitai, S.T. (1983). Disfacilitation and long-lasting inhibition of neostriatal neurons in the rat. *Exp. Brain Res.* *51*, 227–235.

Zohary, E., Shadlen, M.N., and Newsome, W.T. (1994). Correlated neuronal discharge rate and its implications for psychophysical performance. *Nature* *370*, 140–143.